



CHAPTER IV

INTERNAL BUBBLE SHAPES EFFECT ON DIELECTRIC BEHAVIORS IN PVDF FILMS FROM PHASE INVERSION METHOD

4.1 Abstract

In this research, the investigation of the effect of internal bubble shapes (spherical and ellipsoidal) induced in PVDF films on dielectric behavior was focused. The cellular and sponge-like microporous PVDF films were fabricated by phase inversion technique. Then porous films were uniaxially stretched to a final elongation 100% at 90°C for changing internal pores from spherical to ellipsoidal shape. The amount and types of solvent, temperature conditions, and PVDF concentrations were varied in order to investigate the effects of bubbles content, shape of bubbles and structure of film on the dielectric properties. The results showed that at high frequency the dielectric constant of ellipsoidal bubble shape (draw shape) is higher. Moreover, dielectric loss of ellipsoidal bubble shape is still lower than spherical bubble shape. The measured dielectric constant is fitted well with Yamada model indicating 0-3 connectivity of Air/PVDF composites.

Keywords: Poly (vinylidene fluoride); Microporous films; Phase inversion; Dielectric materials; Bubble shapes

4.2 Introduction

In recent years, cellular and porous polymers are interested by researchers. Therefore, a novel concept of creating internal bubbles is introduced by the charge accumulate in bulk of non-polar polymer. However, Poly(vinylidene fluoride) (PVDF) is well known polar-polymer materials for acoustic transducers such as air-bone, water-bone for sound applications and underwater hydrophone devices because of their wide bandwidth, high sensitivity, good electromechanical properties, low power requirements, high generation force, chemical resistance, flexibility, and toughness. In the case of underwater hydrophone device, PVDF films need to add bubbles inside for light weight applications, low acoustic (close acoustic match of water) and mechani-

cal impedance [Lines M E and Glass A M 1979]. A novel concept of creating internal bubble is introduced cellular or porous polymer films which contain partial discharges inside in order to produce gas in the bubbles to achieve improved electrical properties of non-polar polymer such as PP [Neugschwandtner *et al.* (2001)]. The concept is very interesting but not many researchers are investigating the space-charge in the cellular PVDF in order to improve the disadvantage of PVDF film.

Microporous PVDF films are often prepared by immersion precipitation method, in which a polymeric casting is immersed in a nonsolvent bath to induce a phase separation. After drying, liquid phase is removed and left the pores inside membrane called porous membrane [Howe-Grant, M.(1993)]. The variation of membranes with cellular, spongy, and spherulitic structures are controlled by many parameters such as polymer concentrations, dope, bath composition, precipitation temperature, additives, and etc [E. Quartarone *et al.* (2002)].

In this research, the effect of internal bubble shapes on dielectric behavior was studied. The bubble was created inside PVDF films by thermal phase inversion. In this method, PVDF powder was mixed with 3 different chemicals; *N,N* Dimethylacetamide(DMAc), *N,N*-Dimethylformamide(DMF), and Triethylphosphate (TEP) to obtain different microstructures of spherical bubbles. The bubble-shape was changed to ellipsoidal by stretching porous films. Subsequently, internal bubble shapes were observed using Scanning Electron Microscopy (SEM). The dielectric constant and the loss tangent of porous PVDF films were measured as a function of frequencies in the range of 1 kHz-10 MHz at room temperature by impedance/gain-phase analyzer in different % porosity, structure, and bubbles shapes.

4.3 Experimental

A. Materials

The PVDF used was a commercial product (Solvay 1008). *N,N*-Dimethyl acetamide (DMAc, 99.5%), *N,N*-Dimethyl formamide (DMF, 99.8%) were purchased from Lab Scan Co., Ltd. and Triethylphosphate (TEP, 98%) was obtained from Fluka Co., Ltd. All chemicals are used without further purification.

B. Preparation of Porous PVDF films

In the thermal phase inversion method, PVDF 20 (%wt) powder was mixed with 3 different solvents; *N, N*-Dimethylacetamide (DMAc), *N, N*-Dimethylformamide (DMF), and Triethylphosphate (TEP). The different microstructures of spherical bubbles such as cellular and sponge were obtained. After that, the bubble-shape was changed to ellipsoid by stretching the porous films.

C. Preparation for Dielectric and Piezoelectric Measurement

A stretching process typical stretch ratio 1:1, the sample is stretched up to one times its original length by Universal Testing Machine (LLOYD LRX) with Heater Chamber in order to control temperature in system, the ellipsoidal shape of internal bubble can be obtained. And then, subject the sample to large and enduring electric fields (for typical poling conditions, the electric field is approximately 50 kV/mm).

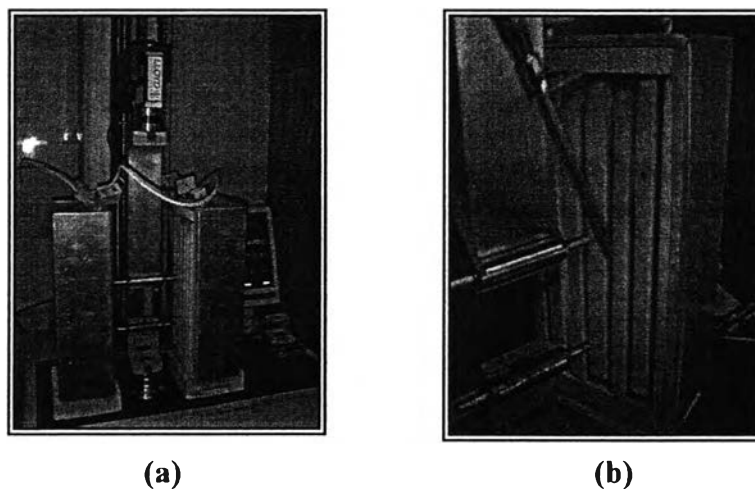


Figure 4.1 The heater band equipment for stretching in PVDF films.

D. Characterizations

The distribution of bubbles in PVDF and morphology of porous PVDF films were observed using scanning electron microscope (SEM; JSM-5200, JEOL). A crystal phase and structure of porous film PVDF were analyzed by X-ray diffraction (Rigaku, model Dmax 2002). The effect of bubbles on temperature decomposition of

PVDF film was investigated by TGA (Perkin Elmer). Finally, the dielectric properties of the specimens of different structure, porosity, shape of bubbles were measured using Hewlett-Packard 4194A impedance/gain phase analyzer. The measurements were performed at room temperature with a frequency range of 1 kHz-10 MHz.

4.4 Results and Discussion

A. *Physical Properties*

Porous PVDF films by phase inversion process have thickness in range of 0.1564-0.1298 mm, opaque, and smooth surface. Although, the photographs of 3 films seem to be the same (Figure 4.2), but the SEM micrograph reveals that 3 different solvents, Dimethylacetamide (DMAc), Dimethylformamide (DMF), and Triethylphosphate (TEP) yield different morphology of porous inside PVDF film.

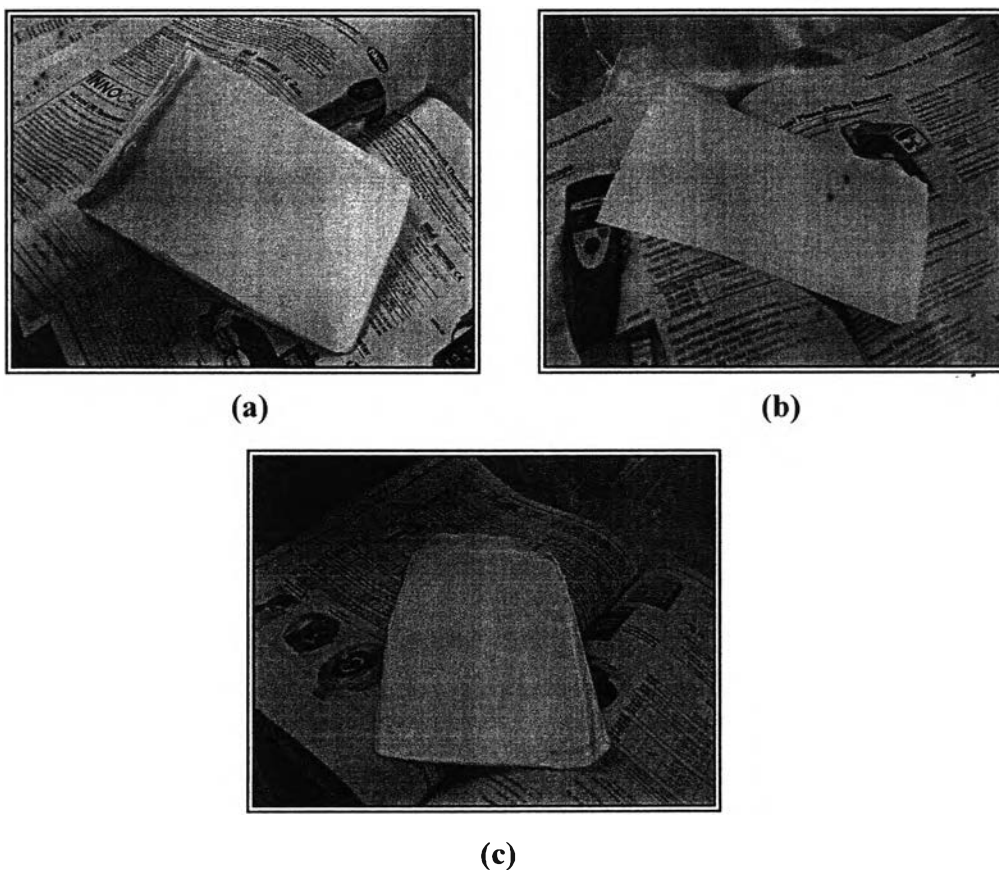


Figure 4.2 Photographs of porous PVDF films obtain from phase inversion technique by (a) DMAc (b) DMF, and (c) TEP.

In phase inversion process, the micro-structure of the films depends on preparation conditions; such as operating temperature, coagulation temperature, polymer concentration and solvent. The cross-sections of porous PVDF films were freeze-fractured under liquid nitrogen, and then samples were gold sputtered and analyzed.

The SEM image shows the cross-section of Porous PVDF films produced by phase inversion technique as following

4.4.1 Scanning electron microscopes-SEM

This studies have been carried out the making of flat symmetric porous PVDF by varying many parameters such as operating temperature, coagulation temperature, solvent , polymer concentration as following;

a) Effect of operation temperature

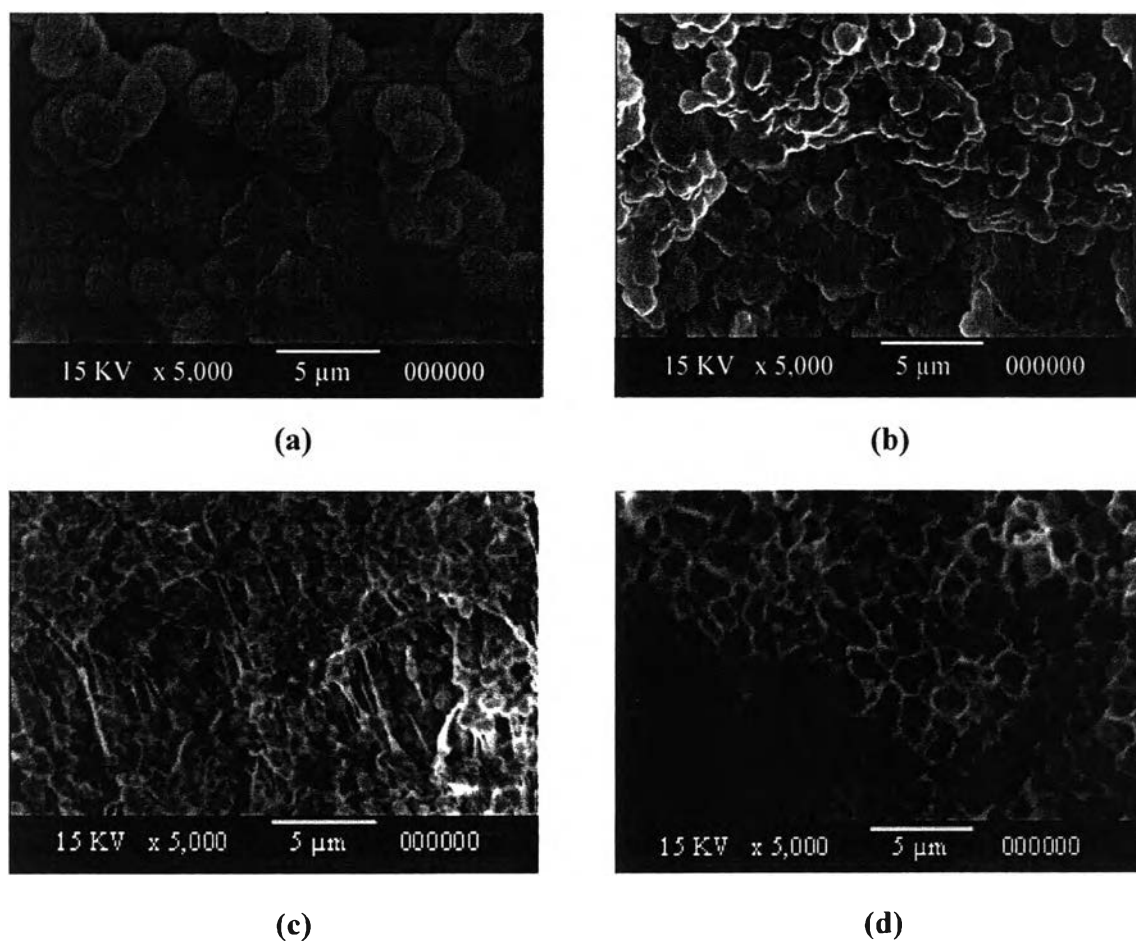


Figure 4.3 SEM micrographs of porous PVDF film by operating T° at (a) 25, (b) 40, (c) 80, and (d) 120°C.

In different operating temperature also effect on the morphology and pore structure that shown in Figure 4.3. PVDF films have morphology like a droplets or globules (polymer rich phase) when prepared by dissolving PVDF with solvent at (a) 25°C (no heat), (b) 40°C, and (c) 80°C until homogeneous. Conversely at (d) 120°C has a cellular pore inside PVDF film (polymer poor phase), due to “a phase diagram” of an upper critical solution temperature which at a higher temperature the solution is still homogeneous. For entropic reasons, many polymer-solvent systems also phase separation at term temperature close to the atmospheric boiling point of solvent.

b) Effect of temperature in coagulation bath

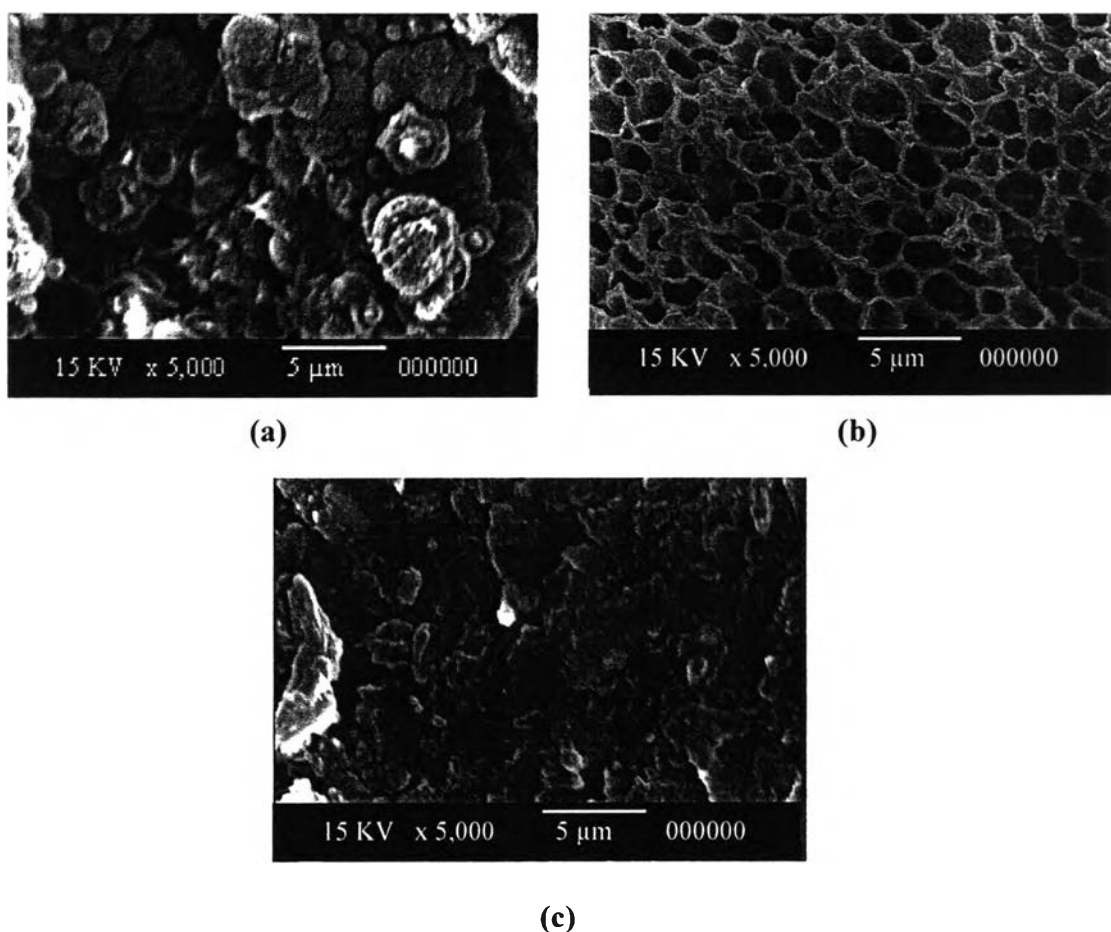


Figure 4.4 Porous structure of PVDF films in coagulation bath at (a) 10, (b) 25 and (c) 50°C, respectively.

The coagulation temperature seems to have an influence on the precipitation rate for PVDF systems. The distill water was used for phase inversion reaction and also, temperature in coagulation bath was varied. Figure 4.4 shows experiments at

three different temperatures 10°C, 25°C, and 50°C. When PVDF was precipitated at lower temperatures (10°C), the cooling rate was high with a strong crystallization potential yielding the phase separation occurred in the unstable region (SD) which enhanced droplets to grow. When quenching at room temperature, the cooling rate was lower and the spherulite size increased, became more regular size in meta-stable region. Due to the longer polymer crystallization time, the droplets were inhibited and the solvents were rejected and the small pores were obtained. The spherulite growth rate of PVDF was extremely high at 50°C, as polymer solvent had enough time to congregate, while the obtained structure and size of pores was largely decreased.

An increasing in the coagulation temperature seems to have a continually decreased of average pore size and porosity was observed.

c) Effect of solvent

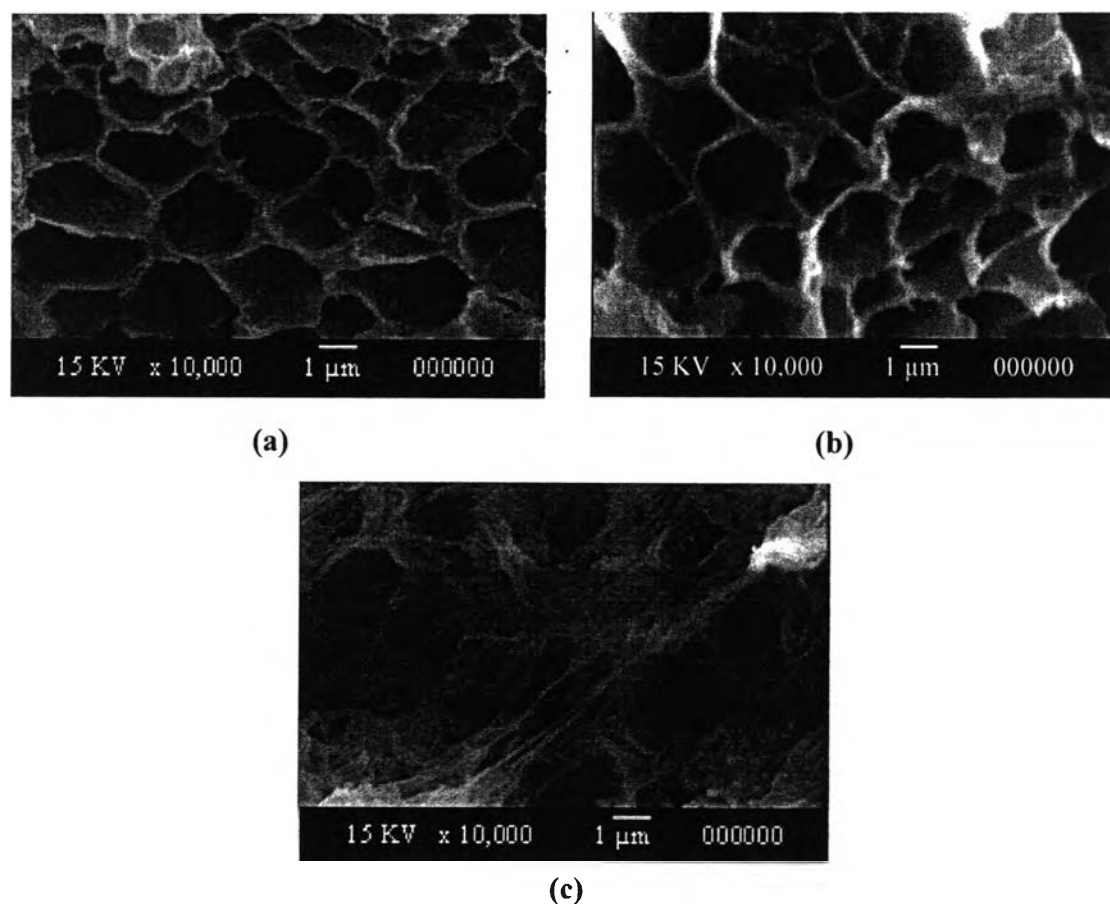
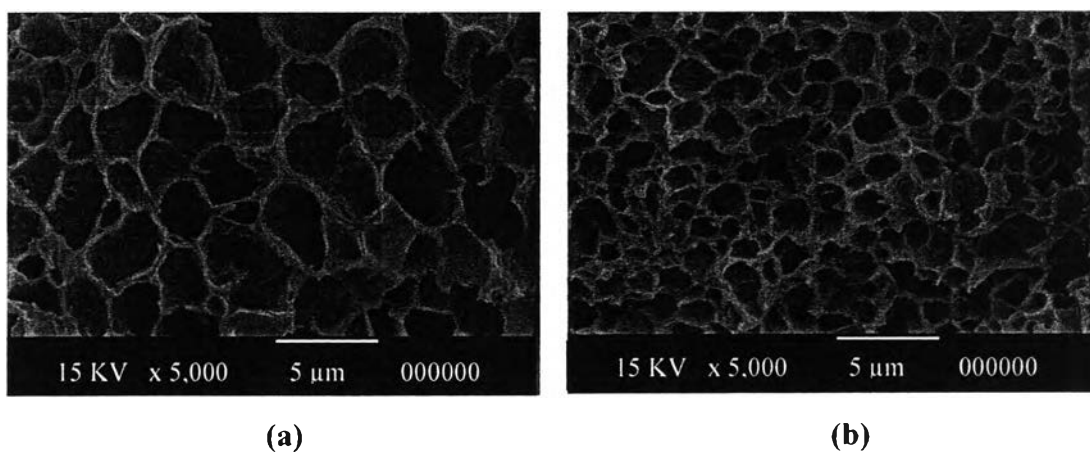


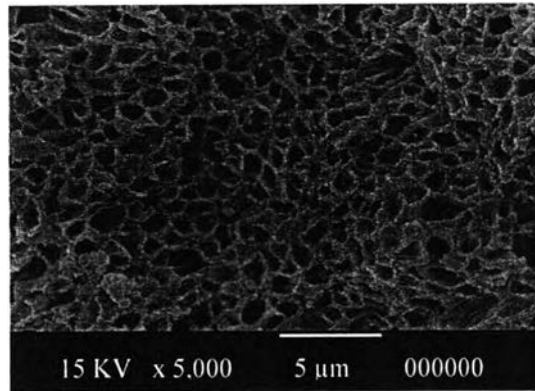
Figure 4.5 Comparison of PVDF microstructures formed in 3 different solvents (a) DMAC, (b) DMF, and (c) TEP.

There were found that PVDF polymer was dissolved quite easily in DMAc and DMF. On the other hand PVDF hardly to dissolves in TEP because of polarity of the solvent. M. L. Yeow, (2003) described the rank solvent power that DMAc > DMF > TEP. Figure 4.5 shows the effects of different solvents on the porous structure of PVDF films; a typical asymmetric cellular structure with some cavities and porous spherical shape beneath the skin layer were exhibit in DMAc and DMF solutions. Also the structure of the TEP casted porous PVDF films exhibited asymmetry sponge structure. Because of its weak solvent power, the minority presence of the non-solvent was sufficient to induce the phase inversion of the polymer solution. These can be suggested that the different structure of porous films depends rather on solvent-water interaction during immersion of thin films into coagulation bath, than PVDF/solvent interaction. The weak interaction of PVDF and water is dominant in controlling the exchange between solvent and coagulant (distill water).

D. Effect of polymer concentration

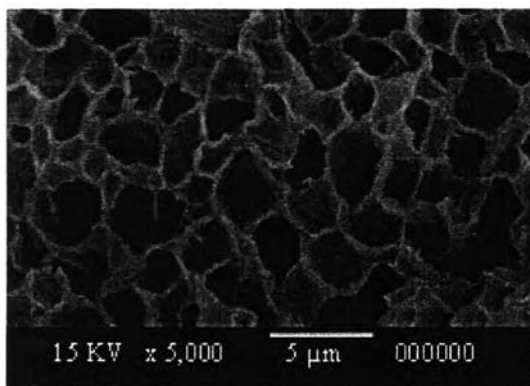
In the phase inversion process, PVDF concentration (%wt) is one of the most important parameter affected on structure, pore size and porosity of PVDF films as presented in Figure 4.6, 4.7, and 4.8. At a higher polymer concentration, the lower pore size was exhibited which provides the tight structures of porous PVDF films.



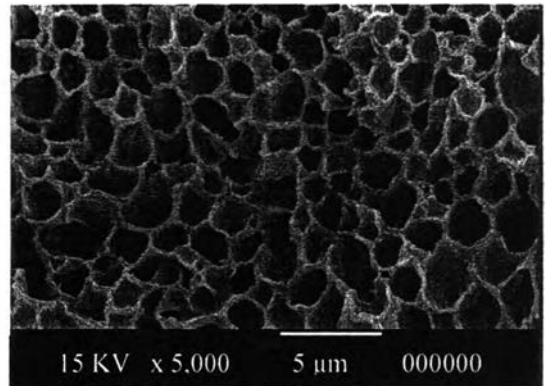


(c)

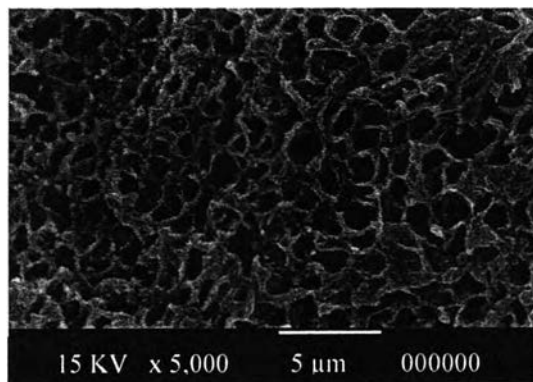
Figure 4.6 SEM micrograph of cross-section of porous PVDF film cast from different polymer concentration (a) 10 (b) 20 and (c) 30 %wt by DMAc.



(a)



(b)



(c)

Figure 4.7 SEM micrograph of cross-section of porous PVDF film casting from different polymer concentrations (a) 10 (b) 20 and (c) 30 %wt by DMF.

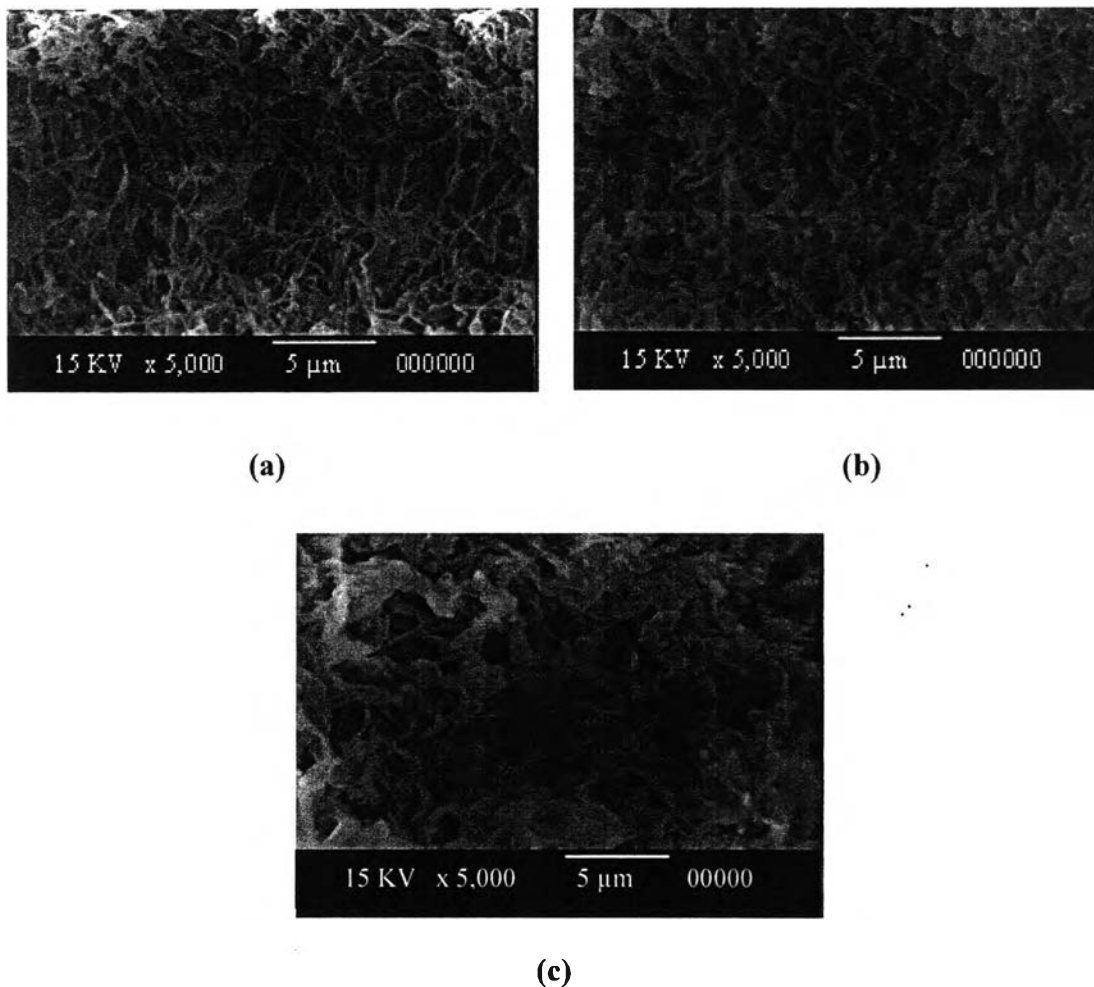


Figure 4.8 SEM micrograph of cross-section of porous PVDF film casting from different polymer concentrations (a) 10 (b) 20 and (c) 30 %wt by TEP.

From the SEM micrograph shown that 30% PVDF concentration has smaller pore size of PVDF film than those from 10% and 20%, while larger pore radius size were fabricated from lower polymer concentration. At higher polymer concentration than 30 %, the interaction between macromolecule starts to interfere and becomes a gel-like.

Finally, porous PVDF films were prepared by isothermal immersion precipitation of a PVDF/DMAc, PVDF/DMF, and PVDF/TEP from distill water bath. The asymmetric structures of the three different porous PVDF films were observed by

SEM micrograph. The SEM image shows cross-section of porous PVDF films produced by phase inversion technique dissolved in different solvents, as seen in Figure 4.9.

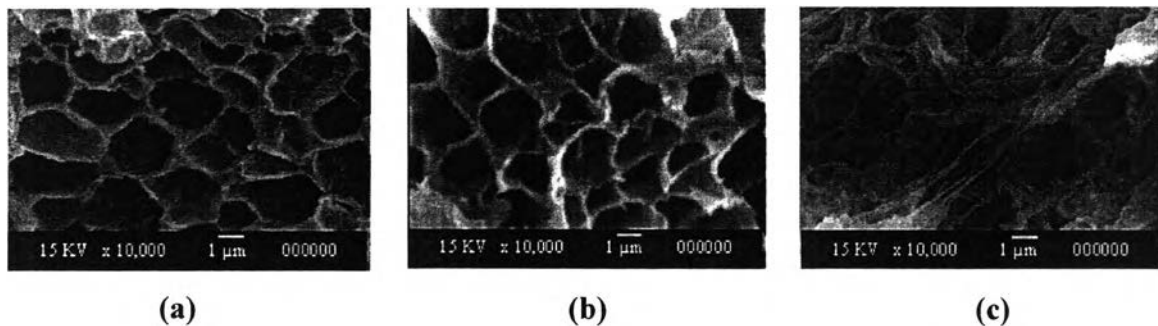


Figure 4.9 Micrographs of cross section of porous PVDF prepared with systems of different solvent.

From SEM micrograph in Figure 4.9 shows that, DMAc and DMF have the same morphology as a typical asymmetric cellular structure with porous spherical shape beneath the skin layer. Also the structure of the TEP casted porous PVDF films exhibited asymmetry sponge-like structure.

To study the effect of bubbles shapes on dielectric behavior in porous PVDF films, the films were stretching in ratio 1:1 (100% elongation) by UTM machine in chamber 90°C. The schematic deformation of pore shapes before and after uniaxially stretched of PVDF films are displayed in Figure 4.10.

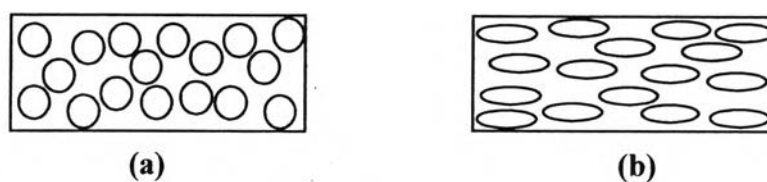
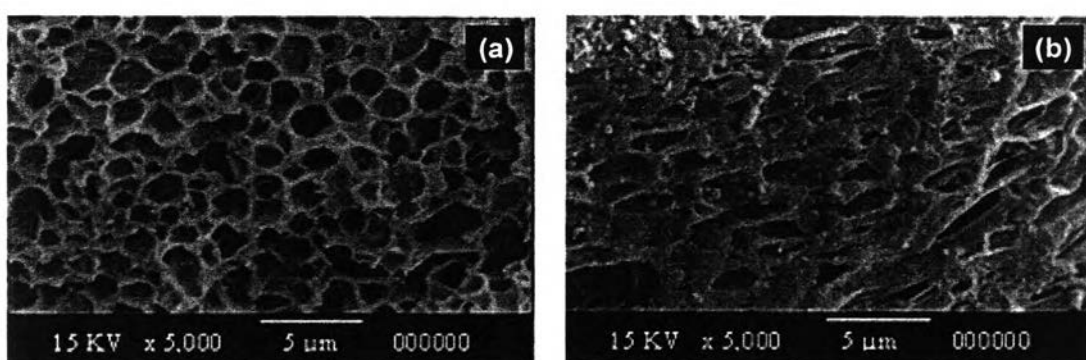


Figure 4.10 The schematic drawing of spherical and ellipsoidal in porous PVDF films.



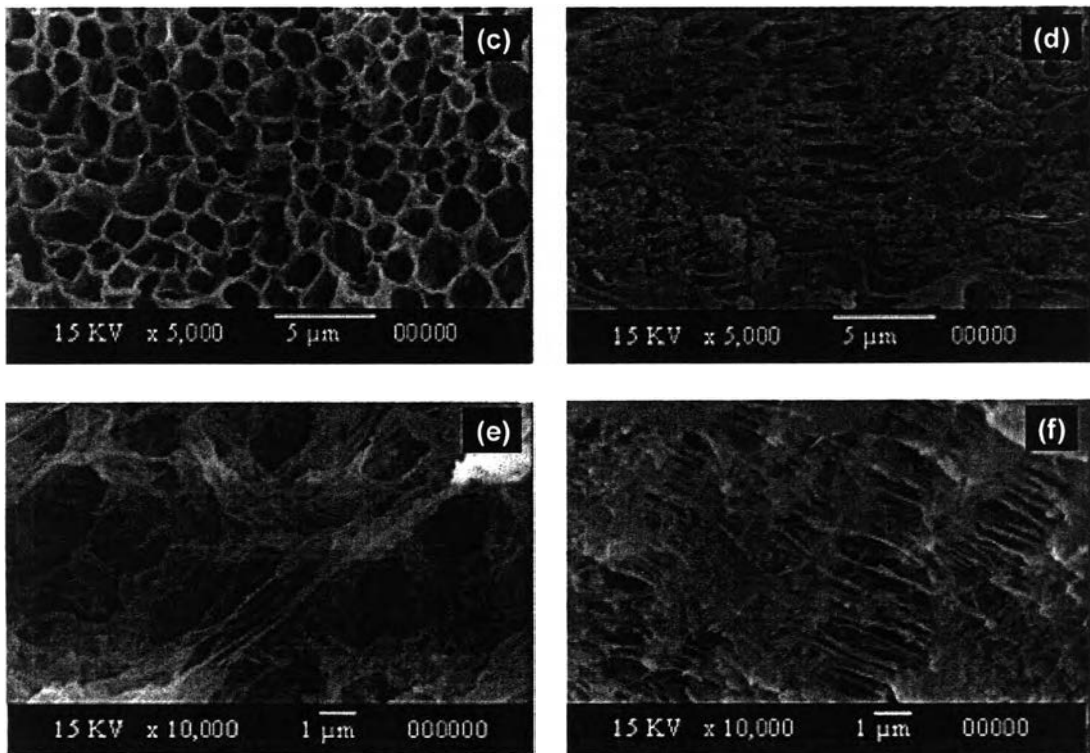


Figure 4.11 Structure of unstrained (spherical) and strained (ellipsoidal) of PVDF diluents systems with PVDF fraction of 20 wt% in (a),(b) DMAc, (c),(d) DMF, and (e),(f) TEP.

The SEM images confirm that the ellipsoidal structure was generated in stretched PVDF films. Figure 4.11 show spherical shape or non-stretching (a) DMAc, (c) DMF, (e) TEP and ellipsoid shape with stretching 100% elongation (b) DMAc, (d) DMF, and (f) TEP.

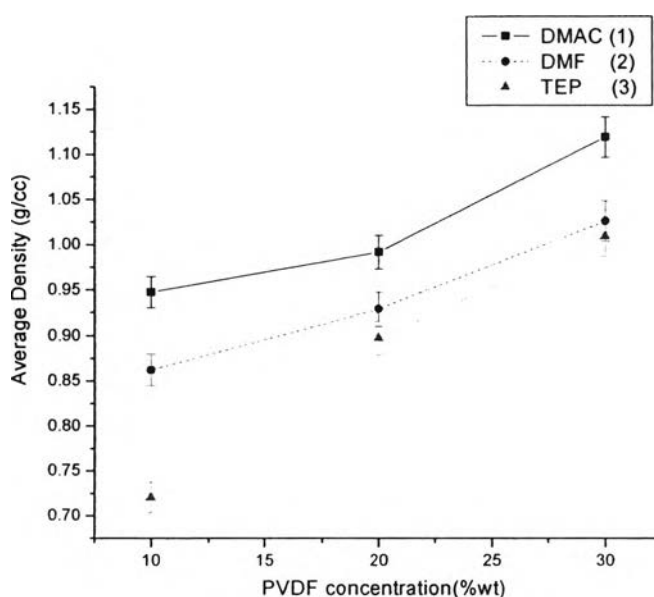
4.4.2 Density of porous films

The apparent densities of porous PVDF film are measured by Pycnometer (Quantachrome, Ultrapycnometer 1000) under helium purge and operated conditions at following:

- Cell size: Small
- V added-small: 12.4138 cc
- V cell: 20.8798 cc
- Target Pressure: 17 psi
- Deviation Achieved: +/- 0.0219
- Maximum Runs: 20
- Number of Runs Averaged: 3

Table 4.1 The Comparison between Density of Non-porous and Porous PVDF film

Sample	Average Density(g/cc)
Non-porous PVDF films	1.7894
Porous PVDF films by DMAC	0.9917
Porous PVDF films by DMF	0.9290
Porous PVDF films by TEP	0.8974

**Figure 4.12** Density of porous PVDF films by (a) DMAc, (b) DMF, and (c) TEP.

In Figure 4.12 porous PVDF films from TEP solvent have a lowest density, due to their sponge-like structure. While the cellular structures, from DMAc and DMF solvent, have a higher density. As shown in Table 4.1, the phase inversion yielded porous PVDF (20%wt) films in different system of solvent. The density of the film was approximately 0.89-0.99 g/cc which obtained by Ultracycrometer 1000. As expected, the density of the porous film is lower than that of non-porous film (1.78 g/cc) due to the penetration of air inside the films which is suitable for light weight applications such as air bone and water bone.

4.4.3 Pore diameter of Porous films

The average pore sizes of porous PVDF films can be determined by using program SemAfore 5.00 JEOL in SEM. The effects of polymer concentration and solvent on pore size were shown in the following Table.

Table 4.2 Average pore diameter of PVDF diluents systems with PVDF fraction 10 %wt

Sample	Average pore diameter (μm)
PVDF with DMAc	2.4911 (Min.1.49, Max.3.75)
PVDF with DMF	1.9987 (Min.0.79, Max.3.02)
PVDF with TEP	1.4452 (Min.0.68,Max.2.55)

Table 4.3 Average pore diameter of PVDF diluents systems with PVDF fraction 20 %wt

Sample	Average pore diameter (μm)
PVDF with DMAc	1.3406 (Min.0.56, Max.2.04)
PVDF with DMF	1.1049 (Min. 0.41,Max. 1.85)
PVDF with TEP	0.7965 (Min.0.32,Max.1.44)

Table 4.4 Average pore diameter of PVDF diluents systems with PVDF fraction 30 %wt

Sample	Average pore diameter (μm)
PVDF with DMAc	0.9924 (Min.0.60, Max.1.79)
PVDF with DMF	0.6513 (Min.0.23, Max.1.66)
PVDF with TEP	0.4784 (Min.0.23, Max.0.77)

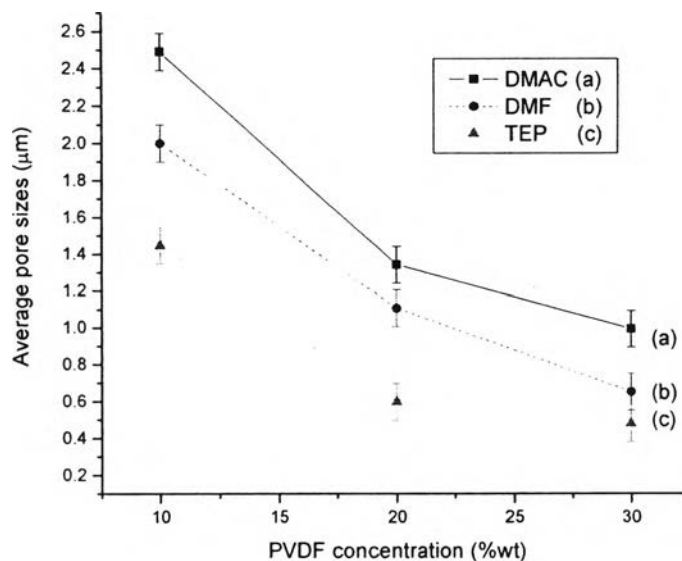


Figure 4.13 Average pore sizes of porous PVDF films in different solvent and polymer concentration.

In Figure 4.13 reveals that a lower polymer concentration 10% has higher average pore sizes of 1.44-2.49 μm . On the other hand, at a higher concentration of polymer exhibited lower average pore size in the range of 0.47-0.99 μm . The solvent shows much effect of pore size which DMAc and DMF produced higher pore size in structure of cellular. Conversely, TEP can yield a smallest of pore size in a sponge-like structure because the polarity of the solvent in TEP lowers than DMF and DMAc.

4.4.4 Porosity measurement of PVDF films

The porous PVDF films were immersed in iso-butanol around 24 hr then taken them out to remove iso-butanol on the surface before weighing and calculating the porosity that available in the literature [Minghao Gu. Gu *et al.* (2006)].

Table 4.5 Porosity of porous PVDF films by different solvent (thickness 120 μm)

Sample	PVDF (wt%)	Average % Porosity
Porous PVDF films by DMAc	20	62.34
Porous PVDF films by DMF	20	68.02
Porous PVDF films by TEP	20	71.04

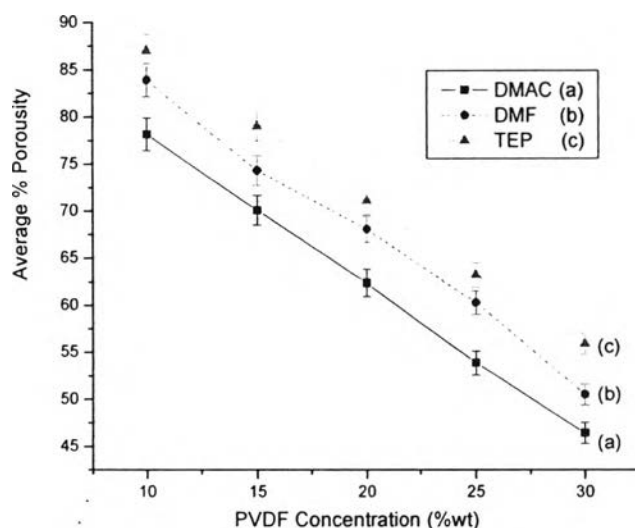


Figure 4.14 Relationship between PVDF concentration and % porosity.

The linear relationship between PVDF concentration in different types of solvent and % porosity was shown in Figure 4.14. The porosity of PVDF films decreased as the concentration of PVDF in solvent increased by comparing between sponge-like and cellular structure, the sponge-like shows higher % porosity than those of cellular structure. Due to the solvent has a close polar with PVDF and strong interaction of C=O with -F- in PVDF, the lower numbers of porosity was produced.

4.4.5 Thermal property analysis-TGA

The thermal properties of various microporous PVDF films with different polymer concentrations and porosity percentages can be determined by TG-DTA. Also, its can be used to make sure that solvent is no longer contaminated in the films. If solvent contaminated, the peak of thermograms will show a steps more than one as shown in the following Figure 4.15;

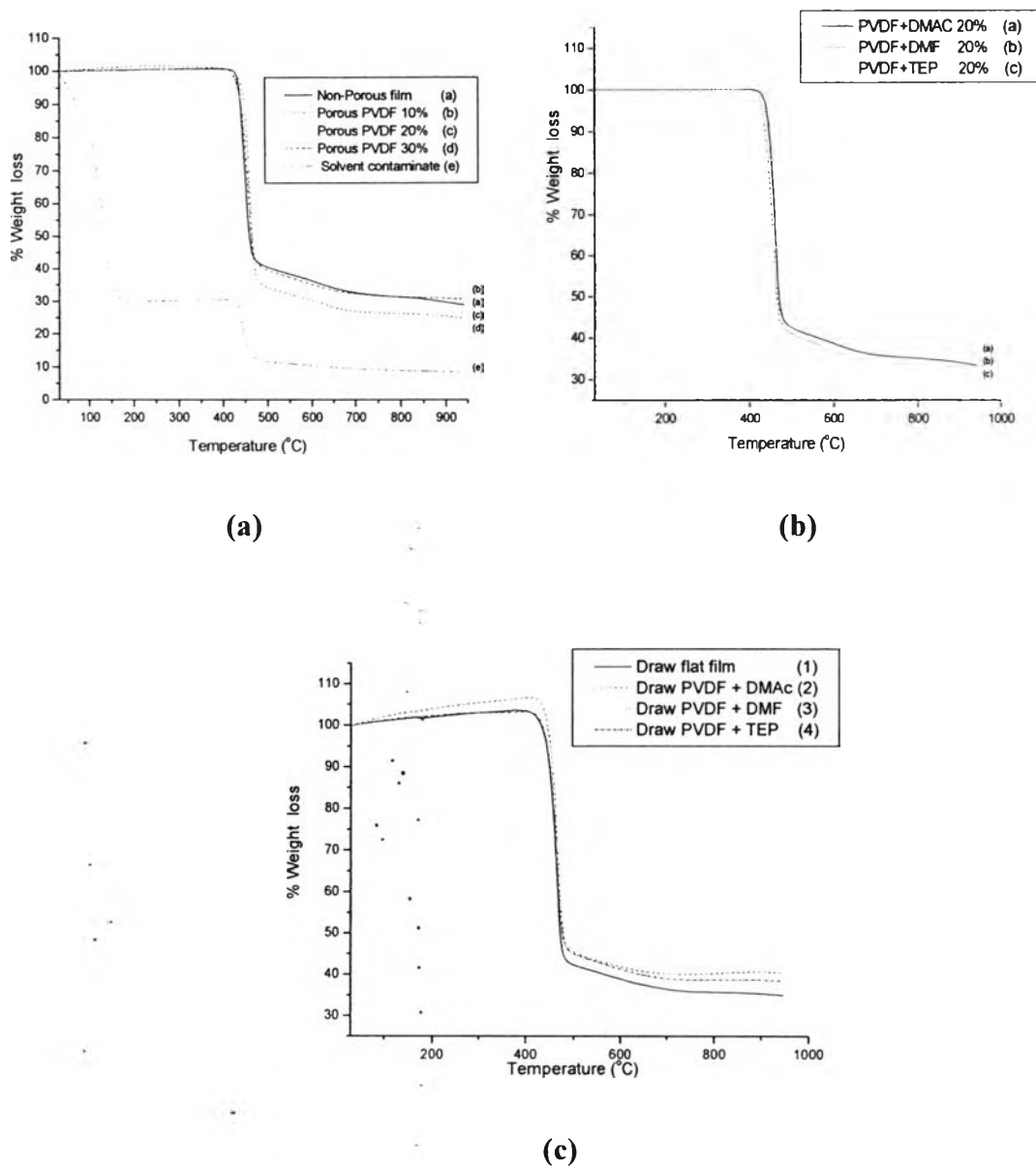


Figure 4.15 TGA thermograms at $10^{\circ}\text{C}/\text{min}$ of nitrogen atmosphere of porous PVDF films in (a) different weight proportions (10, 20 and 30 %wt) (b) different solvent and different structure, (c) different bubble shapes.

Figure 4.15 shows decomposition temperature of different porous structure (cellular and sponge-like structure), porosity or amount of air and shape of bubbles has a similar in range $448.6\text{--}449.3^{\circ}\text{C}$. From all TG-DTA results, can be suggested that the amount of air penetrated, type of porous structure, and stretching (1:1 ratio) does not effect on decomposition temperature (T_d) of porous PVDF films.

4.4.6 Melting behavior -DSC

The melting and crystallization behavior, as measured by DSC, of porous PVDF films shown in Figure 4.8 was carried out in the temperature range between 30-300°C corresponding to the melting point of PVDF (168-170°C). Differential scanning calorimetry (DSC) results indicated the melting temperatures of porous and non-porous have not been changed. And the mechanical stretching does not affect the melting temperature of the films.

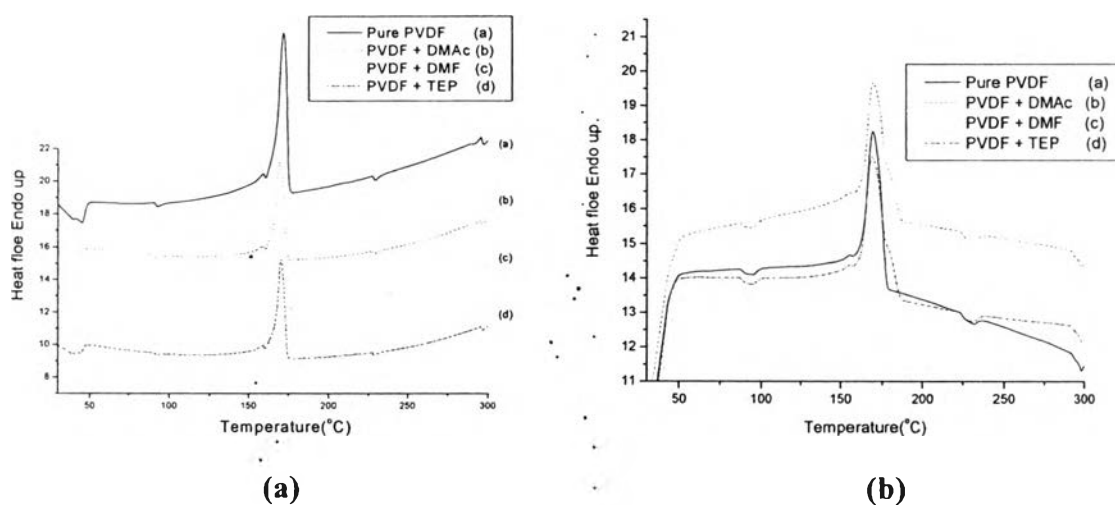


Figure 4.16 DSC thermograms of porous PVDF Films which have (a) spherical and (b) ellipsoid shapes in different solvent system.

In Figure 4.16 (a), the crystallinity of the nonporous PVDF film is 51 % and porous PVDF films from DMAc, DMF and TEP solvent abruptly increase to 58 %, 56 % and 52 %. This can explain from the fact that the high polar solvent has higher orientation than low polar solvent PVDF. In Figure 4.16 (b), crystallinity increases with draw ratio increases that crystalline of the unstretched nonporous PVDF film is abruptly increases up to 64.79 %. For the crystallinity of porous PVDF films by DMAc, DMF, and TEP were slightly increased to 61.67 %, 60.58 %, and 57.23 %, respectively. Stretching of PVDF film facilitates the higher orientation and yields the higher crystallinity.

4.4.7 Infrared spectra analysis-FT-IR

The FT-IR spectra of PVDF films have two major phases (α and β phase) [Rollik, D., *et al.* (1999)]. The characteristic absorption bands of β -phase shows at 509 (CF_2 bending) and 839 (CH_2 rocking) cm^{-1} while α phase shows at 532 (CF_2 bending), 612, 763, and 970 cm^{-1} which were investigated by Salimi, A. and Yousefi, A. A. (2004) and Kim, B. S., *et al.* (1998). Absorption bands of PVDF films are used to calculate the changes in the β crystalline phase by Beer-Lambert law. Appearance of absorption band at 763 and 840 cm^{-1} , feature of α and β crystalline phases, % β -phase content of different solution-crystallized solvent and flat film can be calculated and shown in Table 4.6. The DMF, DMAc solution-crystallized film gives small absorption bands of β application because PVDF molecule were dissolved in a high polar solvent, molecule can be separated between positive and negative charges which provide high polarization yielding high piezoelectric and dielectric properties. However, flat film PVDF show lower β phase spectrums but higher than TEP (all Trans) because molecules can not be separated between each other that shown in Figure 4.17.

A. Porous PVDF films (Spherical bubble shape)

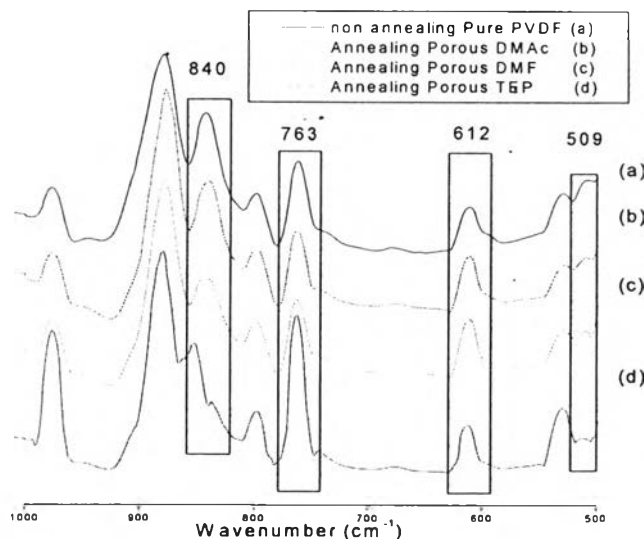


Figure 4.17 FT-IR spectra of (a) Pure PVDF and porous PVDF with (b) DMAc, (c) DMF and (d) TEP solution-crystallized.

Table 4.6 The variations of $F(\beta)$ % of solution-crystallized PVDF system

Material	β -phase content, $F(\beta)$ (%)
Pure PVDF	49.36
Porous PVDF + DMAc solution	52.43
Porous PVDF + DMF solution	50.80
Porous PVDF + TEP solution	45.21

Thus, the effect of polymer concentration or porosity on $F(\beta)$ % content was found that $F(\beta)$ at polymer concentration 10%, 30% nearly value of 20% at all different solvent. Also, the average $F(\beta)$ % of porous films by DMAc, DMF, and TEP are 52.43%, 50.80%, and 45.21%, respectively.

B. Porous PVDF films (Ellipsoidal bubble shape)

A transformation mechanism of α to β crystalline phase was reported as the necking region commences. Necking signs the transformation from spherulitic structure to a micro fibrillar one. This mechanism induces all-trans planar zigzag conformation (β crystalline phase) into the crystals [Mohammadi, B., *et al.* 2007].

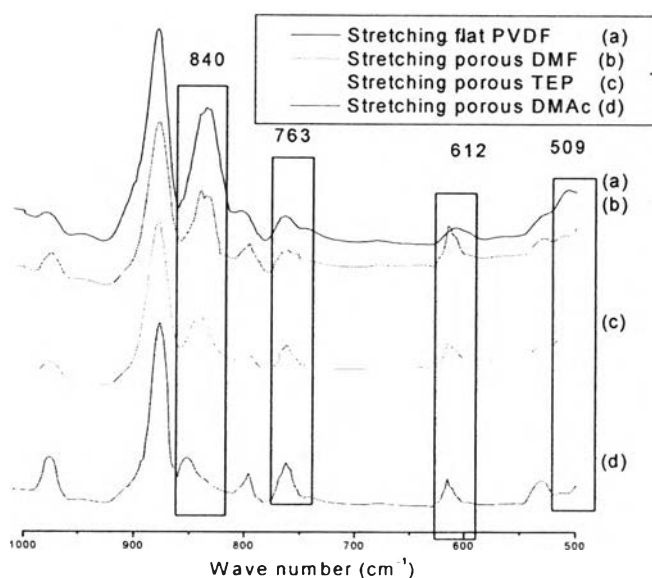


Figure 4.18 FT-IR spectra of stretching (a) flat PVDF and porous PVDF with (b) DMAc, (c) DMF and (d) TEP solution-crystallized.

Table 4.7 The variations of $F(\beta)$ % of stretching PVDF films at solution-crystallized system

Material	β -phase content, $F(\beta)$ (%)
Stretching flat PVDF	77.65
Porous PVDF + DMAc solution	62.96
Porous PVDF + DMF solution	60.71
Porous PVDF + TEP solution	58.44

The complete predominated for β crystalline phase (all-trans) is found in drawn sample. According to Figure 4.18, as draw flat and porous PVDF films (1:1 ratio) the intensity of the characteristic of the α crystalline phase decreases whereas the characteristic of the β crystalline phase increases. Even at stretching of porous PVDF films, the bands at 763 cm^{-1} are quite observable, indicating that α crystalline phase was decreased in the sample. The β crystalline phase content ($F(\beta)$) was calculated for drawn flat PVDF is 77.65%. The calculated $F(\beta)$ of solution-crystallized porous PVDF films in DMAc, DMF, and TEP are summarized in Table 4.7. For high polar solution-crystallized, PVDF have a high value of $F(\beta)$ is observed, The $F(\beta)$ increases as the draw ratio increase.

The calculated % $F(\beta)$ of stretching porous PVDF films is not influence on polymer concentration or porosity, but it increases as the draw ratio increases. For high polar solution-crystallized, PVDF have a high value of % $F(\beta)$ is observed.

4.4.8 β -Phase characterization-XRD

In porous PVDF films, the broad XRD peak implies the mixing of crystalline and amorphous region that show in Figure 4.19. All porous PVDF films exhibited a similar diffraction pattern. The diffraction peaks at 20.1° , 26.7° are (1 1 0), (0 2 1) planes of α -phase structure [Kohpaiboon, K., and Manuspiya, H., (2007)], while 37° is (1 1 1), (2 0 1) plane of β -phase structure. The curve fitting of amorphous and crystalline region in XRD was calculated yielding crystallinity of porous films from DMAc, DMF, and TEP to 20.48, 19.84, and 19.68 %, respectively [Ye, Y., 2004].

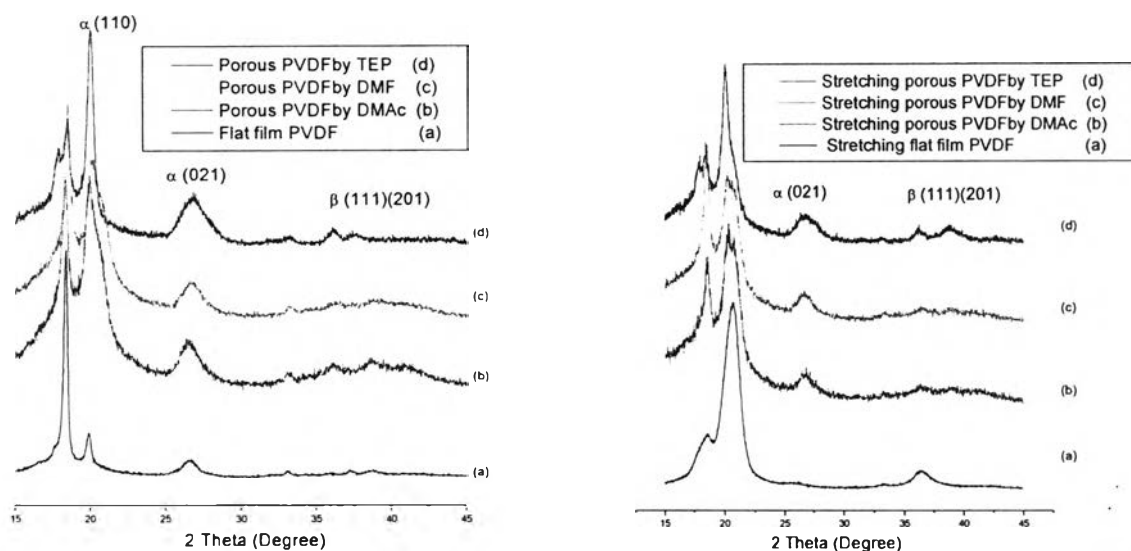


Figure 4.19 XRD diffractograms of (a) non-stretching and (b) stretching porous PVDF films prepared by different solvents system: DMAc, DMF, and (d)TEP.

In Figure 4.19 (b) show the α -phase no longer exist and peak of β -phase was appeared when the film was stretching. The effect of stretching porous PVDF films on % β crystallites that occurred in 30.76%, 28.04%, and 27.12%. The % β crystallinity of nonporous and porous PVDF film can be improved by stretching.

B. Electrical Properties

4.4.9 Dielectric measurement (LCR Meter)

4.4.9.1 *Dielectric properties of non-porous PVDF*

The dielectric properties of nonporous PVDF film were shown in Figure 4.20. From the result, the stretching film has higher dielectric constant than nonstretching film due to the increasing of oriented molecule (β -phase) in stretched film. From these results, they were clear that PVDF film exhibited dielectric relaxation with frequency. High loss was observed at higher frequency.

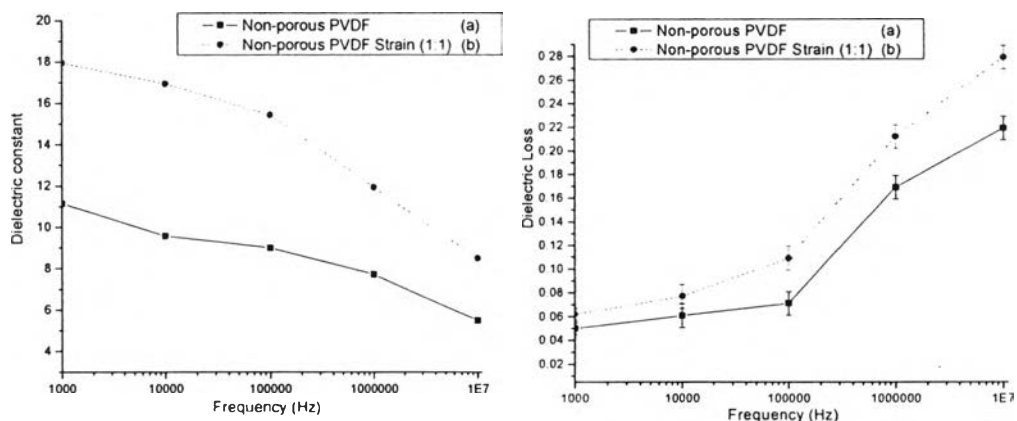


Figure 4.20 Comparing between (a) non-strained and (b) strained of non-porous PVDF films.

4.4.9.2 Dielectric properties of Porous PVDF

a) Effect of structure in porous PVDF films

Figure 4.21 shows the variation of dielectric constant and the loss tangent with applied electric field of porous PVDF films at different structure. The higher dielectric constant was observed in cellular structure which produced by DMAC than sponge-like structure by TEP, but all porous structures are still lower than flat PVDF film. The reason might arise from the existence of air trap or porosity in films. However, the loss tangent in all porous films are lower than flat film.

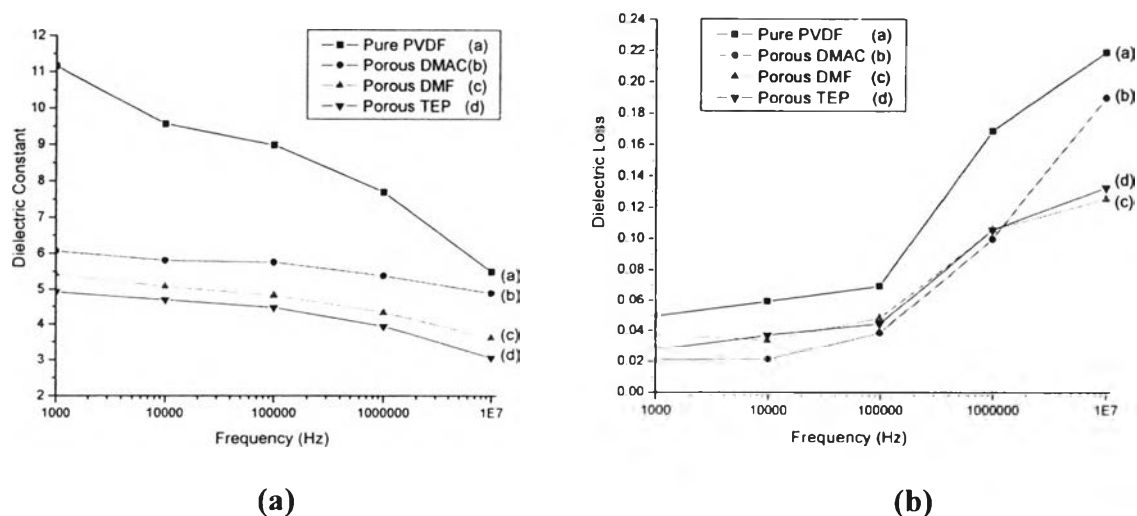


Figure 4.21 The frequency dependence of (a) the dielectric constant dielectric and (b) loss tangent of flat and porous PVDF films at different morphology structures.

b) Effect concentration of PVDF 10, 20, and 30 (%wt)

The effects of porosity or polymer concentration on dielectric constant and loss tangent of the porous PVDF films were also investigated. Figure 4.22, 4.23, and 4.24 shows the variation of dielectric constant of the porous PVDF with frequency at 1 kHz- 10 MHz which fabricated by DMAc, DMF, and TEP, respectively. From this graph, it should be observed that the dielectric of PVDF films decreased with increasing air content.

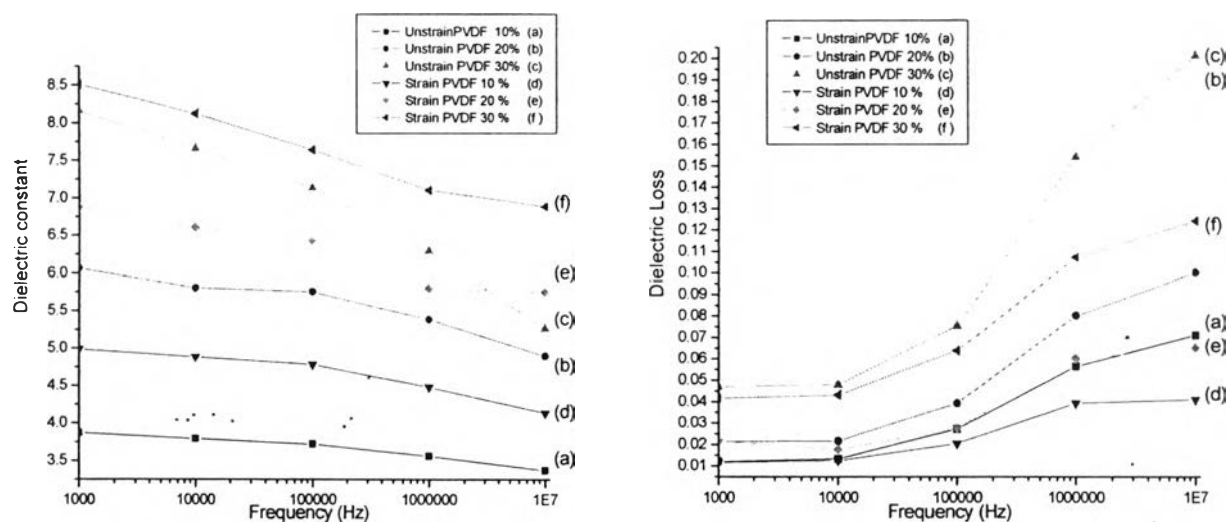


Figure 4.22 The frequency dependence of the (a) dielectric constant and (b) dielectric loss tangent with frequency at room T ° of porous PVDF films by DMAc at in different % weight of polymer and different shapes.

It is obviously noticed that the value of dielectric constant increases with increasing polymer concentration from 10 to 30% of PVDF/Air ratio. As the weight fraction of PVDF is added up to 30%, the dielectric constant of the film shows the highest value. The dielectric loss decrease with increasing air bubbles which can be seen that 30% polymer concentration shows higher loss tangent than 10% at various frequencies due to the bubbles can absorb energy around the surface. Nevertheless, all weight proportions of porous films are lower than 0.2 at frequency up to 10 MHz.

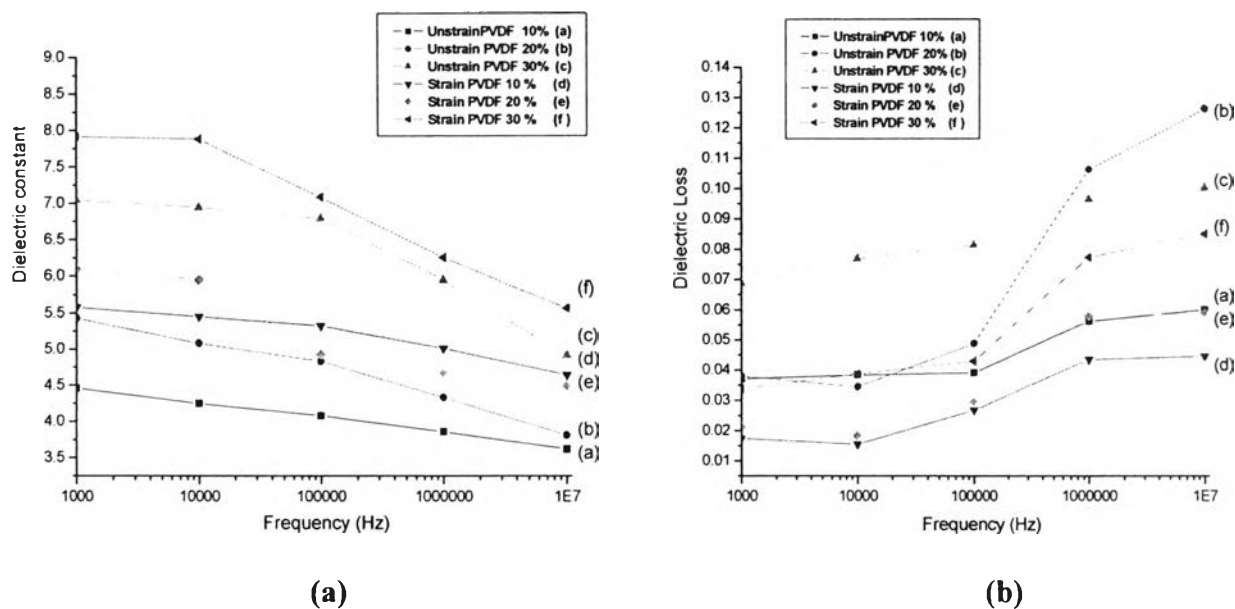


Figure 4.23 The frequency dependence of the (a) dielectric constant and (b) dielectric loss tangent with frequency at room T ° of porous PVDF films by DMF at in different % weight of polymer and different shapes.

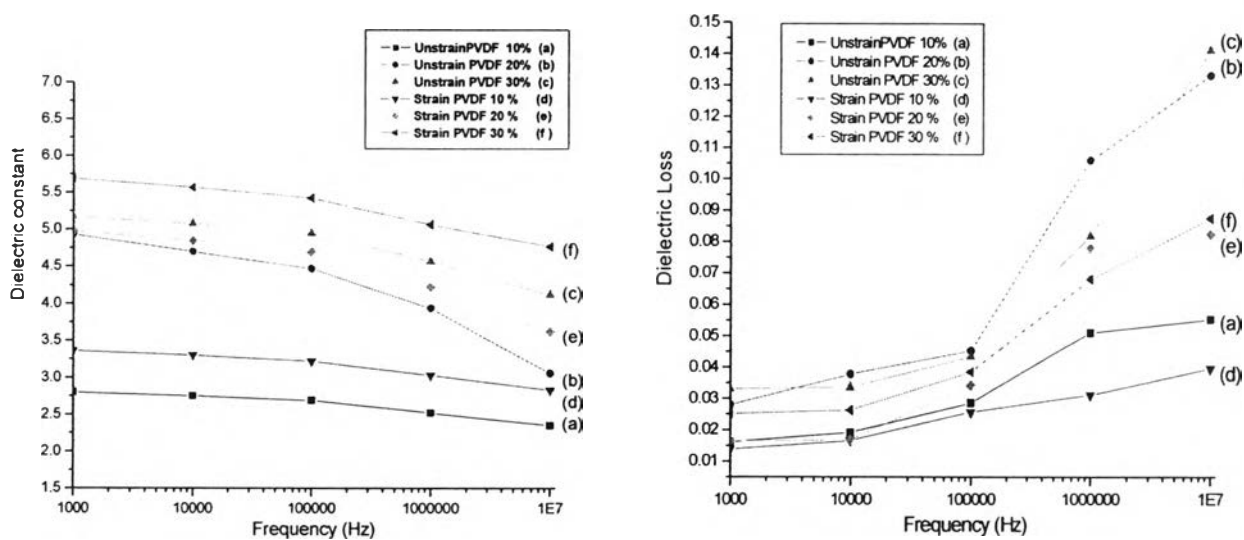


Figure 4.24 The frequency dependence of the (a) dielectric constant and (b) dielectric loss tangent with frequency at room T ° of porous PVDF films by TEP at in different % weight of polymer and different shapes.

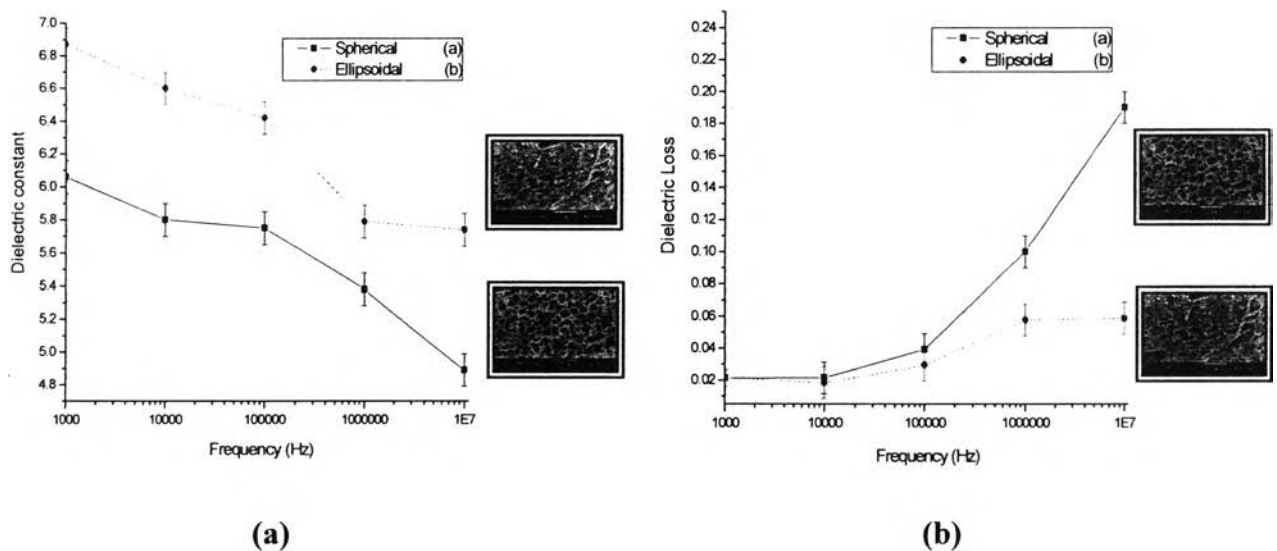
The dielectric constant slightly decreased with increasing frequency, which referred to frequency independence behavior. The cause of this phenomenon is

dipolar polarization in polymer matrix decreased caused by the delay in molecular polarization with respect to a changing frequency in a dielectric medium.

c) Effect of bubbles shapes in dielectric and loss tangent

When the air bubbles were induced inside the film from the evaporation of solvents, the dielectric constant of PVDF is lower. The bubble shapes were classified into spherical and ellipsoidal shape. The dielectric of ellipsoid bubbles shape inside PVDF films is higher than those of spherical shape for all air compositions. By stretching a spherical bubble into elliptical, the random charges were oriented and separated between positive and negative charges providing higher charge density and strong dipole moment.

This result could be explained by interfacial polarization inside the PVDF / air composites in applied alternating field. The dielectric constant dependent frequency shows less effect in porous PVDF films. Also, the loss tangent of PVDF is lower than 0.2 at all frequencies as shown in Figure 4.25.



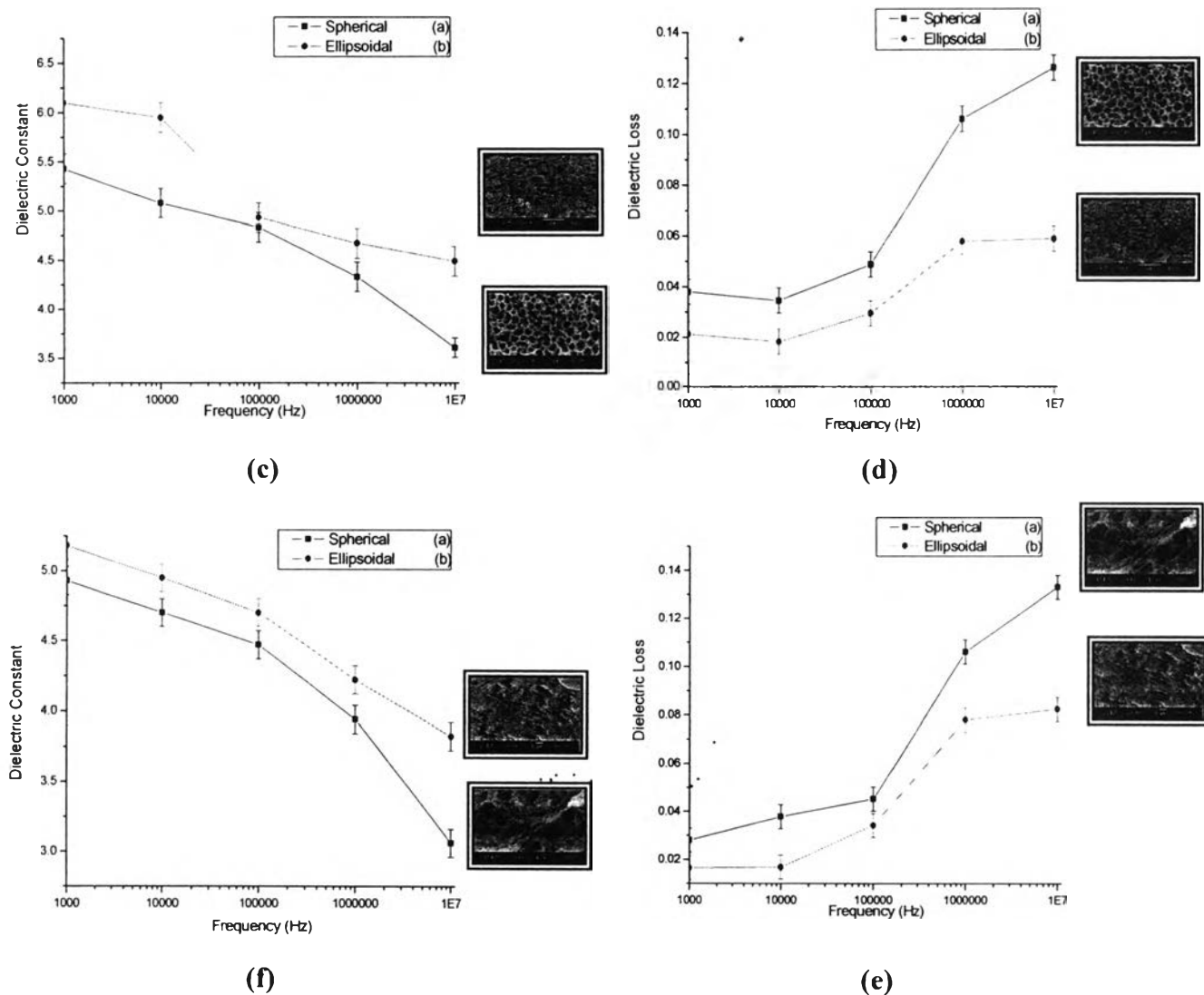


Figure 4.25 Frequency dependent (a),(c),(e) dielectric constant and (b),(d),(f) dielectric loss of porous PVDF films with different shape between spherical and ellipsoidal shape; (a),(b) from DMAC solvent, (c),(d) from DMF solvent and (e),(f) from TEP solvent.

4.4.10 Connectivity of composites (Air/PVDF)-Experimental Data Fitting

Four theoretical mixing models for 0-3 connectivity have been proposed in order to calculate the dielectric constant of the composites comparing with experimental results, including Yamada model, Bruggeman formulae, Lichtenecker model, and Kerner expression modified by Jayasundere-Smith (J-S prediction), as shown in Figure 4.26 and 4.27 for spherical and ellipsoidal shape. The equations of these models are described as follow: [Liou, J.W., and Chiou, B.S. (1998)], [R. Popielarz and C. K. Chiang (2001)]

Yamada model:
$$\varepsilon = \varepsilon_p \left[\frac{\eta \phi (\varepsilon_c - \varepsilon_p)}{\eta \varepsilon_p + (\varepsilon_c - \varepsilon_p)(1 + \phi)} \right] \quad (4.1)$$

Lichtenecker model:
$$\log \varepsilon = \log \varepsilon_p + \phi \log \left(\frac{\varepsilon_c}{\varepsilon_p} \right) \quad (4.2)$$

Bruggeman formulae:
$$\frac{\varepsilon_c - \varepsilon}{\varepsilon_c - \varepsilon_p} \left(\frac{\varepsilon_p}{\varepsilon} \right)^{1/3} = 1 - \phi \quad (4.3)$$

Kerner expression:
$$\varepsilon = \frac{\varepsilon_p \phi_p + \varepsilon_c \phi_c [3\varepsilon_p / (\varepsilon_c + 2\varepsilon_p)] [1 + 3\phi_c (\varepsilon_c - \varepsilon_p) / (\varepsilon_c + 2\varepsilon_p)]}{\phi_p + \phi_c (3\varepsilon_c) / (\varepsilon_p + 2\varepsilon_c) [1 + 3\phi_c (\varepsilon_c - \varepsilon_p) / (\varepsilon_c + 2\varepsilon_p)]} \quad (4.4)$$

Where ε is the dielectric constant of the composites, ε_p and ε_c refer to the dielectric constants of the polymer matrix and the internal bubbles, respectively, ϕ is the volume fraction of air and η is a shape parameter. For the calculation, the dielectric constant of air ($\varepsilon_c = 1$) and the pure poly(vinylidene fluoride) ($\varepsilon_p = 11$) were used. The dielectric constants were measured at room temperature ($\sim 25^\circ\text{C}$) and 1 kHz [T. Yamada, T. Ueda, and T. Kitayama, (1982)].

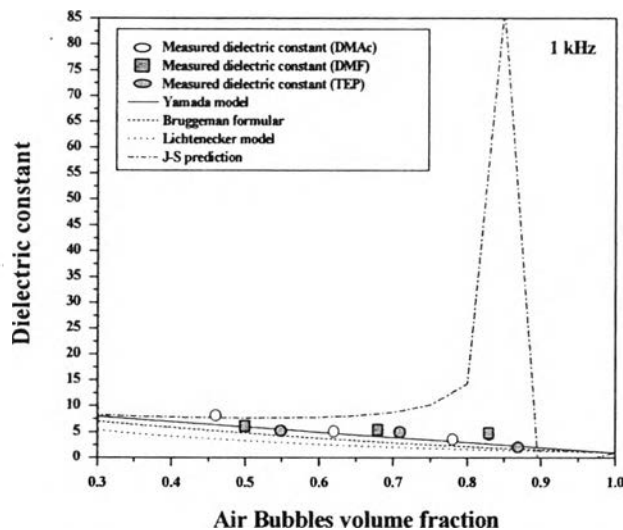


Figure 4.26 Plot of theoretical models and the measured dielectric constant for spherical shape at room temperature and 1 kHz.

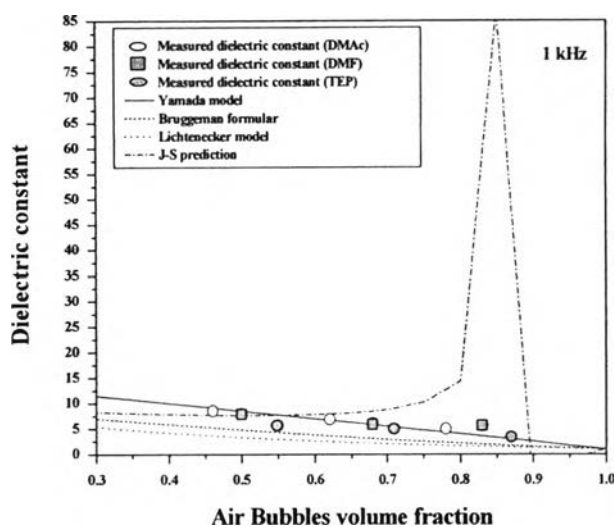


Figure 4.27 Plot of theoretical models and the measured dielectric constant for ellipsoidal shape at room temperature and 1 kHz.

From the comparison between the measured dielectric constants and theoretical models, it can be seen from Figure 4.26 that the measured dielectric constants of the PVDF spherical bubbles composites are higher than those calculated from Bruggeman formula and J-S prediction. While the value calculated from Lichtenecker model was higher than the measured dielectric constants. Among these theoretical models, the measured dielectric constants of spherical shape and ellipsoidal shape agree well with the theoretical prediction based on Yamada model indicating 0-3 connectivity.

4.5 Conclusions

The microporous composites of PVDF/air bubbles can be prepared by phase inversion process, with the optimized temperature of 120°C and precipitated in ambient T°. The morphology of porous can be classified into cellular (DMAc, DMF) and sponge-like (TEP) structures with lower density that would be suitable for sound applications and underwater hydrophone. The amount of air penetrated, type of porous structure, and stretching (1:1 ratio) does not effect on decomposition (T_d) and melting (T_m) temperature in porous PVDF films but slightly effect on β -phase.

This study shows that the dielectric constant of PVDF films with ellipsoidal bubble shape shows more promising data including higher dielectric constant, less

relaxation with frequency and lower loss tangent than spherical shape. The ellipsoidal shape caused a stronger dipole moment; results in a higher dielectric than those of spherical shape. Dielectric constant of both spherical and ellipsoidal bubble shapes in PVDF film are not less than 5 at 1 kHz, and loss tangent is less than 0.02 for all air fractions. The dielectric constant of the composites in different air shapes between spherical and ellipsoidal follows the mixing rule by Yamada model.

4.6 Acknowledgements

The authors would like to thank Dr. Pitak Laoratanakul and MTEC staffs for useful assistance and instrument for characterizations. The partial funding of research work was provided by Polymer Processing and Nanomaterials Research Unit.

4.7 References

- A. Bottino *et al.* (2006) Novel porous membranes from chemically modified poly(vinylidene fluoride), Journal of Membrane Science, 273 (2006) 20–24.
- A. J. Lovinger.(1982) Poly(vinylidene fluoride) in Developments in Crystalline Polymer Apply Science, Publisher, p.185.
- E. Quartarone *et al.* (2002)Transport Properties of Porous PVDF Membranes Journal of Physic Chem. B, 106, 10828-10833.
- Kim, B. S., Lee, J.Y. and PorTer, R.S.(1998) The Crystalline phase Transformation of Poly(Vinylidene Fluoride)/Poly(vinyl Fluoride) Blend Films, Polymer Engineering And Science, 38(9), pp 1359-1365.
- Kohpaiboon, K.,and Manuspiya, H.,(2007). 0-3 Connectivity of PVDF/BST Piezo-electric Composites M.S. thesis, The Petroleum and Petrochemical College, Chulalongkorn University, Bangkok, Thailand.
- P. Sajkiewicz; A Wasiak; Z Gocłowski. (1999) Phase transitions during stretching of poly(vinylidene fluoride) European Polymer Journal, 35, 423±429.
- P. van de Writte *et al.*(1996) Phase Separation Process in Polymer Solutions in Relation to Membrane Formation membranes Journal of Membrane Science, 117, 1-31.
- Howe-Grant, M.(1993),Membrane technology. Encyclopedia of chemical Technology, 16, 135-192.

- Justin E. George. (2007) Piezoelectric Sensing Capabilities of Polyvinylidene Fluoride: Application to a Fluid Flow through a Compliant Tube Aerospace Engineering Texas A&M University, Class.
- Liao-Ping Cheng. (1999). Effect of Temperature on the Formation of Microporous PVDF Membranes by Precipitation from 1-Octanol/DMF/PVDF and Water/DMF/PVDF Systems Macromolecules, 32, 6668-6674.
- Liou, J.W., and Chiou, B.S. (1998). Dielectric tenability of barium strontium titanate/silicone-rubber composite Journal of Physics: Condense Matter, 10, 2773-2786.
- Lines M E and Glass A M 1979 Principles and Applications of Ferroelectrics and Related Materials (Oxford:Clarendon).
- Minghao Gu. Gu *et al.* (2006) Formation of poly(vinylidene fluoride) (PVDF) membranes via thermally induced phase separation, Desalination 192 .160–167.
- Mohammadi, B., Yousefi, A.A., Bellah, S. M. (2007) Effect of tensile strain rate and elongation on crystalline structure and piezoelectric properties of PVDF thin films, Polymer Testing, 26, pp 42-50.
- N.E. Frost, P.B. McGrath, and C.W. Burns,(1996) Effect of fillers on the dielectric properties of polymers, IEEE International Symposium on Electrical Insulation, pp. 300-303.
- Neugschwandtner *et al.* (2001) Piezo- and pyroelectricity of a polymer-foam space-charge electret, Journal of applied physics, 89, 8.
- R. Popielarz and C. K. Chiang (2001), Polymer Composites with High Dielectric Constant Macromolecules, 34, 5910–5915.
- Rollik, D., Bauer, S. and Gerhard-Multhaupt, R. (1999) Separate contributions to the pyroelectricity in poly(vinylidene fluoride) from the amorphous and crystalline phases, as well as from their interface, Journal of Applied Physics, 85(6), pp 3282-3288.
- S.H. Xie, B.K. Zhu, X.Z. Wei, Z.K. Xu, and Y.Y. Xu, (2004) Polyimide/BaTiO₃ composite with controllable dielectric properties, Composite: Part A, vol. 36, pp. 1152-1157.
- Smolorz, S.; Grill, W. (1995) "Focusing PVDF transducers for acoustic microscopy" Research in Nondestructive Evaluation, Springer-Verlag, New York, NY, USA, Vol. 7, No. 4, pp. 195-201.

- T. Yamada, T. Ueda, and T. Kitayama,(1982) Piezoelectricity of a high-content lead zirconate titanate/polymer composite, Journal of Applied Physics, vol. 53(6), pp. 4328-4332. 1982.
- Ye, Y., Jiang, Z., Wu, Y., Zwng, H., Yang, Y. and Li W (2004) Characterization and Ferroelectric Properties of Electric Poled PVDF Films, School of optoelectronic Information, University of Electric Science and Technology of China.